Vet. Med. Austria / Wien. Tierärztl. Mschr. **95** (2008), 219 - 225

From the Small Animal Surgical Center[1], the Clinical Department of Small Animals and Horses, Clinic of Surgery, Ophthalmology and Veterinary Dentistry[2] and Clinic of Orthopedics in Ungulates[3] (University of Veterinary Medicine, Vienna), the Austria Research Institute for Chemistry and Technology[4], Vienna, and the Upper Austria University of Applied Sciences, Wels Campus, Austria[5]

Finite element modelling of the feline antebrachium - comparison of stress in the intact bones and after extramedullary bridging of a mid-diaphyseal fracture

G.R.F. MAHR[1,2], Ch. HINTERHOFER[3], H. HAIDER[4], K. LORINSON[1], J. KASTNER[5] and D. LORINSON[1]

received November 30, 2007
accepted for publication April 21, 2008

Keywords: finite element model, fracture, osteosynthesis, surgery, radius.

Summary

Application of an interlocking nail (IN) was analyzed to stabilize a simple diaphyseal feline antebrachial fracture. The purpose was to investigate stress distribution during static weight bearing using a finite element model (FEM).

A regularly shaped radius and ulna from a cat of a body mass of 5 kg was used to create a FE foreleg model. A vertical load of 15 N was used for the simulation of a 4-leg static loading. The modulus of elasticity (E) of the bones was assumed 10,000 MPa. A simple and not dislocated fracture was simulated in the middle third of the antebrachial diaphysis. An IN with a length of 68 mm and a diameter of 4 mm was chosen for the stabilization of this fracture. Von Mises stress and strain in the FEM of the intact and fractured bones and the implant respectively were used to compare the selected situations. For better analysis both antebrachial bones were divided into their anatomical regions.

In the intact feline radius, diaphyseal stress values changed from 1.56 MPa to 6.87 MPa from proximal to distal. Ulnal diaphyseal stresses ranged from 0.0811 MPa to 0.0356 MPa (proximal), from 0.0356 MPa to 0.746 MPa (middle) and from 0.746 MPa to 0.356 MPa (distal). In the fractured and stabilized radial diaphysis, values in the proximal third increased from 2.75 MPa to 6.87 MPa and decreased to 0.176 MPa at the location of the second proximal screw. In the middle third of the tended radius where the fracture was located the values were negligibly small (0.0706 MPa) and increased to 6.87 MPa where the proximal of the 2 distal screws was located. In the distal third constant values of 6.87 MPa were found. In the fractured ulna, peak stresses were located in the fractured area in the middle third of the ulna with values between 0.176 MPa and 0.441 MPa.

This FEM may be expected to be the basis for future studies into biomechanics of the feline antebrachium. An extramedullarily applied IN might be a usable tool to treat simple not dislocated diaphyseal fractures of feline radius and ulna.

Schlüsselwörter: Finite Elemente Modell, Fraktur, Osteosynthese, Chirurgie, Radius.

Zusammenfassung

Finite Elemente Modell des Unterarms der Katze – Vergleich der statischen Belastung am intakten Knochen und nach extramedullärer Überbrückung einer Diaphysenfraktur

In dieser Studie wurde der Einsatz eines Verriegelungsnagels zur Stabilisierung einer simplen Fraktur von Radius und Ulna überprüft. Ziel dieser Studie war es, unter Verwendung eines Finite Elemente Modells (FEM) die statischen Belastungsverhältnisse an den Unterarmknochen einer Katze zu untersuchen.

Von einer, aus anderen Gründen als diese Studie, euthanasierten Katze wurden Radius und Ulna entnommen und mittels eines technischen Computertomographen erfasst. Aus den resultierenden Daten wurde das FEM generiert, welches die Basis dieser Studie bildete. Die Belastung einer Vorderextremität einer durchschnittlichen Katze von 5 kg Körpermasse im Stand der Ruhe wurde mit 15 N simuliert und im Bereich der proximalen Knochenenden in vertikaler Richtung angesetzt. Die Materialeigenschaften der Knochen wurden mit einem Elastizitätsmodul (E) von 10.000 MPa und einer Querkontraktionszahl (ν) von 0,3 definiert. Anschließend wurde eine simple Fraktur in der Diaphyse von Radius und Ulna simuliert und diese Fraktur mit einem extramedullär angebrachten Verriegelungsnagel (technische Daten: 68 mm Länge, 4 mm Durchmesser, E = 215.000, ν = 0,29) stabilisiert. Erneut wurde das Modell bedingungsgleich mit 15 N belastet und in der Folge die Werte der Belastung an den stabilisierten Knochen in dem FEM abgelesen und mit den Belastungswerten der intakten Knochen verglichen. Für die Übersichtlichkeit der Analyse wurden die Knochen in ihre anatomischen Regionen aufgeteilt.

Im intakten Radius variieren die Belastungswerte von 1,56 MPa bis 6,87 MPa von proximal nach distal. In der intakten Ulna reichen die Belastungswerte von 0,0811 MPa bis 0,0356 MPa im proximalen Bereich, von 0,0356 MPa bis 0,746 MPa im mittleren Bereich und von 0,746 MPa bis 0,0356 MPa im distalen Bereich. Im frakturierten und mittels Verriegelungsnagels stabilisierten Radius stiegen die Belastungswerte im proximalen Drittel von 2,75 MPa auf 6,87 MPa und fielen dann im Bereich der 2. proximalen Schraube auf 0,176 MPa ab. Im mittleren Drittel des Radius, wo die Fraktur simuliert wurde, waren die Belastungswerte vernachlässigbar klein (0,0706 MPa), stiegen im distalen Drittel im Bereich der 1. distalen Schraube wieder auf 6,87 MPa an und blieben konstant auf diesem Niveau bis zum distalen Ende des Knochens. In der frakturierten Ulna fanden sich im mittleren Drittel, wo die Fraktur simuliert wurde, Spitzenwerte der Belastung von 0,176 MPa und 0,441 MPa.

Diese Studie zeigt, dass sich, berechnet in der Finiten Elemente Methode, der Verriegelungsnagel sehr gut eignet, um simple Diaphysenfrakturen zu versorgen und eine gute Kraftüberleitung zu gewährleisten.

Dieses FEM versteht sich als Basismodell für weitere Studien der Biomechanik des felinen Unterarms und soll einen Akzent setzen, Tierversuche einzuschränken und möglichst zu verhindern, da viele - vor allem technische und biomechanische Fragestellungen - auch auf diesem Weg bearbeitet werden können, Bioverträglichkeitsstudien kann dieses Modell jedoch nicht ersetzen.

Abbreviations: 3 D = three-dimensional; E = Modulus of elasticity; FE = finite element; FEA = finite element analysis; FEM = finite element model; IN = interlocking nail; MPa = megapascal; N = Newton; ν = Poisson's ratio

Introduction

The outcome of surgical procedures is significantly influenced by the understanding of the biological processes underlying the biomechanical functioning of bone, such as bone remodelling and healing. Experimental investigations have been performed in vivo and in vitro, and some of the theoretical investigations have used FEA. This study aimed to create an anatomically accurate, three-dimensional (3D) FEM of the feline antebrachial bones for investigating stress distribution.

FEA - a tool for stress calculations

FEA is a computer-based numerical technique that can be used to calculate the stresses and strains in structural components, including the deflection, stress, vibration, and buckling behaviour. FEA makes it possible to analyze both reversible elastic deformations and plastic deformations (in which the shape of an object is permanently changed). The use of FEA in the analysis of biological models for particle mechanics and membrane functions was first reported in 1969 by MOORE et al., since when it has proven itself to be an indispensable tool in many areas of science, in particular structural and mechanical engineering. The main contribution of FEA to medical science is that it can offer detailed insights into the mechanical properties and dynamical behaviour of tissues, organs, and bones that are impractical in actual experiments with real samples. FEA was first used in veterinary medicine in the early 1970s, to analyze cardiac and vascular structures in dogs (PAO et al., 1974), since when it has increasingly been used in orthopedic research in canines (LAUER et al., 2000; SHAHAR et al., 2003), equines (HINTERHOFER et al., 2001), and bovines (HINTERHOFER et al., 2005, 2006). However, we found no publications on the modulus of elasticity (*E*) or stress and strain distributions in feline antebrachial bones.

Typical small-animal long-bone fracture - the cat foreleg

Fractures of the radius and ulna are a recurrent problem in cats, reportedly representing 7.7 % (VNUK et al., 2004), 18 % (BOUDRIEAU, 2003), and 38.5 % (VNUK et al., 2004) of feline fractures. Up to 64 % (VNUK et al., 2004) of all fractures in cats are due to so-called high-rise syndrome, with other contributors being traffic accidents and other types of blunt trauma. The fractures are reportedly located in the diaphysis in 65.7 % (WENKEL and KAULFUSS, 2001) of all cases, with 17.8 % and 16.5 % being in the proximal and distal metaphysis or epiphysis, respectively (VNUK et al., 2004). The antebrachial fractures are simple, fragmented, and complex in 74 %, 16.4 %, and 9.6 % of cases, respectively (VNUK et al., 2004). Due to the anatomical configuration of the radius and ulna, diaphyseal fractures are difficult to fix with intramedullary pinning. External fixator and plate fixation are the most commonly used osteosynthesis devices in antebrachial fractures (BOUDRIEAU, 2003). In the canine and feline femur, tibia, and humerus, the interlocking nail (IN) represents another successful device for stabilizing diaphyseal fractures of long bones (JOHNSON, 2003).

For the present study we investigated the use of an IN as an innovative method to treat a simple, not-dislocated fracture of the diaphysis of the feline radius and ulna with the aid of FEA. We considered that an IN would be an appropriate tool for minimally invasive surgery in osteosynthesis. We tested this hypothesis by comparing the results of stress analyses of the intact feline antebrachial bones with the outcomes of fractured bones stabilized with an IN. An anatomically accurate FEM of the feline antebrachium was constructed, which represented the antebrachial bones of a cat in a 4-legged stance. The only loading was the bodymass while standing still, muscle forces were ignored, and because the radius is the main weight-bearing bone in the foreleg (ROCHAT and PAYNE, 1993), only the fractured radius was stabilized with an extramedullary IN.

The purpose of this study was to create an anatomically accurate, 3D FEM of the feline antebrachial bones to investigate the stress distribution during static weight bearing. The results of this analysis of simulated forces were compared with the stress distribution present in a simple, mid-diaphyseal antebrachial fracture stabilized with an extramedullary IN.

Material and methods

FEM

A regularly shaped radius and ulna from a 5-kg cat, which was euthanized for reasons other than this study, were dissected from the foreleg. The skin, muscles, tendons, joint capsules, and periosteum were removed manually. All residual organic material was removed with 20 % hydrogen peroxide. The dried bones were then scanned at the Upper Austrian University of Applied Sciences, with a 3D CT scanner (RayScan, 3D, Walischmiller, Markdorf, Germany) and a 225-micron focus tube. The detector of this CT scanner is a 1024×1024-element amorphous-silicon flat-panel matrix detector (RID 1640 AL1 ES, Perkin Elmer Vertriebs GmbH, Vienna, Austria) with a Gadox Scintillator (KASTNER et al., 2006) using a 1-mm aluminium prefilter. The CT data were obtained at a resolution of 115.3 µm. The current and voltage of the tube were 220 µA and 170 kV, respectively, the integration time of the detector was 1 s, and each 360 ° rotation comprised 900 projections. The voxel data from the 3D CT scanner were used for the surface reconstruction, with software (VG StudioMax® ver. 1.2.1, Volume Graphics, Heidelberg, Germany; and Pointmaster®, ver. 4.0, Knotenpunkt, Balingen, Germany) used to reconstruct the surface of the bones on the computer by generating a point swarm (Fig. 1a). This 3D computer-aided-design data set was transferred to the Austrian Research Institute for Chemistry and Technology, where the FEM was built by transferring the point cloud into a complete geometrical FEM. FE meshing was performed using IDEAS® (10 NX series SDRC, Electronic Data Systems, Plano, Texas). The complete model of the intact bones consisted of 38,936 nodes and 21,341 elements (Fig. 1b), and that of the fractured bones stabilized with an IN consisted of 58,241 nodes, with 5,484 elements assigned to the IN and 26,685 elements assigned to the bones (Fig. 2b).

Material properties and loading values

During a 4-legged stance, 60 % of the bodymass rests on the forelegs, and hence each carries 1.5 kg of a 5-kg animal. Therefore, a load of 15 N was used in simulations of the feline FE foreleg model. This load was applied by defining vertical vectors to the proximal joint surfaces of the according bones. The main load acts on the radius, because this bone is the principal weight-bearing bone of the foreleg (ROCHAT and PAYNE, 1993) (Fig. 3a).

The modulus of elasticity of the tested material - which is needed for all FEM calculations - was taken from an appropriate reference: comparable long bones of other species and humans reportedly range from 10,380 MPa to 22,230 MPa (MORGAN et al., 2003). Because of the small dimensions of the feline radius and ulna, we used E = 10,000 MPa. The material was assumed to be isotropic, with a Poisson's ratio of 0.3. Light spring elements were used to combine the radius and ulna in their appropriate positions, and the distal end of the antebrachial bones were restrained in motion to simulate the missing distal extremity. The FEMs of the fractured bones were combined, loaded, and restrained in the same way. In accordance with the literature (RUDD and WHITEHAIR, 1992; WENKEL and KAULFUSS, 2001; BOUDRIEAU, 2003; VNUK et al., 2004), a simple, not-dislocated fracture was simulated in the middle third of the corpus radii and ulnae by taking out a 1-mm slice of bone material in a 45 ° cutting direction to the long run of the bones (Fig. 2a). A single FEM of the feline radius and ulna was used for all calculations.

The implant

An IN with a length of 68 mm and a diameter of 4 mm (product code 11-4.0-068-02-02-2.0, Innovative Animal Products, Rochester, MN) and screws of a diameter of 2 mm were chosen for the stabilization of the fracture. This device was modelled with E = 215,000 N/mm^2 and a Possion's ratio of 0.29 and added to the FEM (Fig. 2b) according to standard surgery. To maintain realism, the fracture of the ulna was also bridged with light spring elements simulating the surrounding soft tissue that would hold the fragments together (Fig. 3b).

Analysis of the FEM

Von Mises stress in the material of the intact and fractured bones and the implant were assessed in the dominant direction according to the equation of RUMPEL and SONDERHAUSEN (1990).

$$\zeta = 1/\sqrt{2}\ \sqrt{(\zeta_x - \zeta_y)^2 + (\zeta_y - \zeta_z)^2 + (\zeta_z - \zeta_x)^2}$$

Both of the bones included in the FEM (the radius and ulna) were divided into their appropriate anatomical regions: caput radii, corpus radii, and trochlea radii for the radius, and olecranon, corpus ulnae, and caput ulnae (including processus styloideus) for the ulna (KÖNIG, 1992; NICKEL et al., 1992; SCHALLER, 1992; FREWEIN and VOLLMERHAUS, 1994). Both the corpus radii and corpus ulnae were additionally divided into proximal, middle, and distal thirds. For interpretation of the stress measured in this feline radius and ulna simulation, measuring points were marked on the pictured intact bones as well as on the stabilized bones to compare the values of the intact bones with those of the broken and stabilized bones (Fig. 4a, b).

The load applied to the model of the intact bones as well as to the model of the broken and stabilized bones was defined by vertical vectors to the proximal joint surfaces. The results were calculated with the von Mises equation and were able to be compared with the corresponding values of the other model.

Trial surgery

We performed a trial surgical procedure parallel to the development of the FEM using a cat that corresponded to the weight assumptions of the FEM, which had been euthanized for reasons other than this study. The foreleg was manually broken and the limb was prepared for surgery. We first attempted to treat the fracture using minimally invasive surgery. A tiny incision was made near the carpal joint on the craniomedial contour of the foreleg right above

Tab. 1: Comparison of the values of stress (in MPa) obtained from the loaded FEMs of the intact and stabilized bones; position 1 represents the proximal end of the bone

Radius	MPa	MPa	Ulna	MPa	MPa
Position	Intact	Stabilized	Position	Intact	Stabilized
1	0.746	0.441	1	0.000104	0.0000456
2	1.56	1.1	2	0.000957	0.00453
3	0.746	1.1	3	0.0185	0.00453
4	1.56	2.75	4	0.0185	0.0283
5	3.28	6.87	5	0.0185	0.0283
6	6.87	6.87	6	0.0385	0.0283
7	6.87	6.87	7	0.0811	0.0283
8	6.87	6.87	8	0.0811	0.0283
9	6.87	0.176	9	0.17	0.176
10	6.87	0.0043	10	0.356	0.176
11	6.87	0.000725	11	0.356	0.176
12	6.87	0.000725	12	0.356	0.176
13	6.87	0.0113	13	0.356	0.176
14	6.87	0.0706	14	0.356	0.176
15	6.87	6.87	15	0.356	0.441
16	6.87	6.87	16	0.746	0.441
17	6.87	6.87	17	0.746	0.176
18	6.87	6.87	18	0.746	0.176
19	6.87	6.87	19	0.746	0.0706
20	6.87	6.87	20	0.746	0.0706
21	6.87	6.87	21	0.746	0.0706
22	6.87	6.87	22	0.746	0.0706
23	1.56	2.75	23	0.746	0.0283
24	0.356	0.441	24	0.746	0.0283
			25	0.356	0.0283
			26	0.356	0.0706
			27	0.356	0.0283
			28	0.356	0.0283
			29	0.17	0.0283

the processus styloideus radii, through which the IN - fixed onto an aiming device - was introduced beneath the skin (Fig. 5a). In this way we verified that there was sufficient space for the insertion of the implant between the bone, soft tissue, and skin in a real animal (Fig. 5b and c). After this trial a standard approach was made as is normally used in traditional osteosynthesis (Fig. 5d). The fracture was reduced and the IN was inserted at the cranial contour of the radius (Fig. 5e). The necessary holes were made with a 1.5-mm drill proximal and distal to the fracture, measured and tapped, and then the IN was fixed with 2-mm screws (Fig. 5f) starting with the most proximal and most distal screws followed by the remaining screws. The screws were tightened, and the cut was sewn.

Results

Measuring points were marked on the radius (n=24) and ulna (n=29) (Fig. 4) to obtain comparable values of stress from the intact and stabilized bones. The values are listed in Tab. 1 and displayed in Fig. 7.

The simulation of the intact feline radius revealed stresses of 0.746 MPa to 1.56 MPa in the area of the caput radii. The stresses increased in the proximal third of the intact radius, from 1.56 MPa to 6.87 MPa. The values in the middle and distal thirds were constant at 6.87 MPa, and decreased from 6.87 MPa to 0.356 MPa in the area of the trochlea radii.

In the simulation of the intact feline ulna revealed stresses up to 0.0385 MPa in the region of olecranon. In the proximal third of the intact ulna exhibited stresses from 0.0811 MPa to 0.0356 MPa. The stresses increased from 0.0356 MPa to 0.746 MPa in the middle third of the intact ulna, and decreased from 0.746 MPa back to 0.356 MPa in the distal third of the intact ulna. In the area of the caput ulnae, the stresses in the processus styloideus decreased from 0.356 MPa to 0.17 MPa.

In the broken feline radius stabilized with an extramedullary IN, the stresses ranged from 0.441 MPa to 1.1 MPa in the area of the caput radii. The stresses increased from 2.75 MPa to 6.87 MPa in the proximal third of the stabilized radius and decreased to 0.176 MPa at the location of the second proximal screw. In the middle third of the stabilized radius, where the fracture was located, the stresses were negligibly small (less than 0.0706 MPa), and are not plotted in the graph. The stresses increased to 6.87 MPa at the location of the proximal of the 2 distal screws, and were constant at 6.87 MPa in the distal third. The values of the area of the trochlea radii decreased from 6.87 MPa to 0.441 MPa.

In the broken ulna the stress was up to 0.0283 MPa in

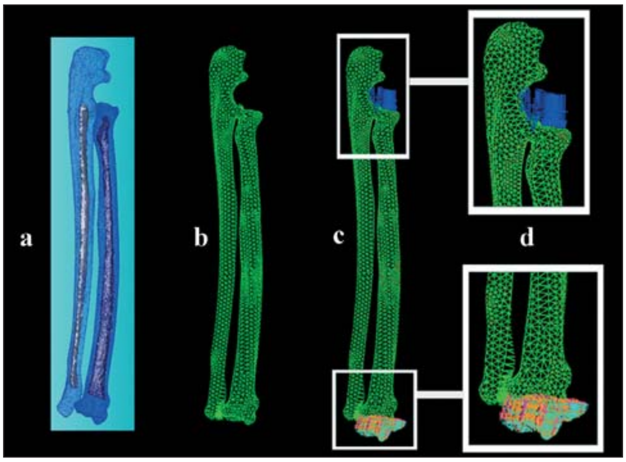

Fig. 1: FEM of the intact bones: (a) point cloud generated from the CT data; (b) combined FEM of the feline radius and ulna; (c) including the boundary conditions; (d) enlarged views of boundary conditions

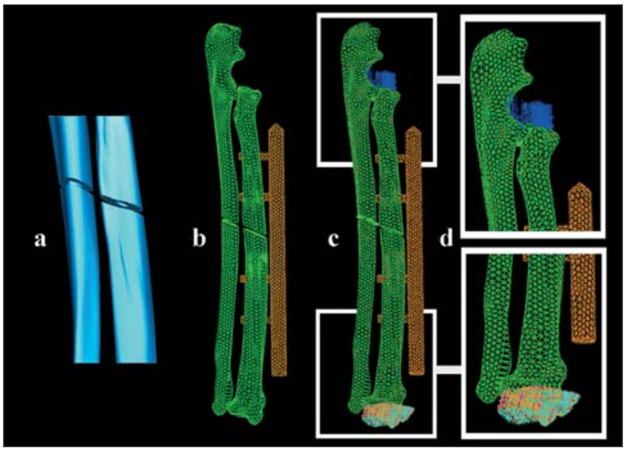

Fig. 2: FEM of the fractured bones: (a) photorealistic illustration of the fractured area; (b) treatment with an extramedullary IN; (c) including the boundary conditions; (d) enlarged views of boundary conditions

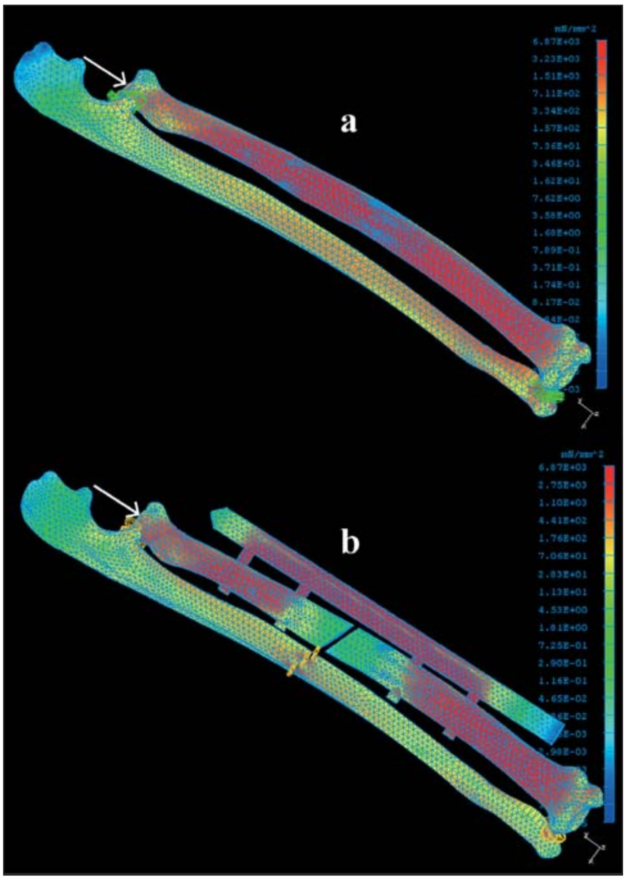

Fig. 3: Screenshots showing (a) the loaded model of the intact feline radius and ulna; (b) the loaded model of the fractured bones stabilized with an extramedullary IN; the white vector marks the direction of pressure load, the colours visualize the amount of stress (red = high stress, blue = low stress).

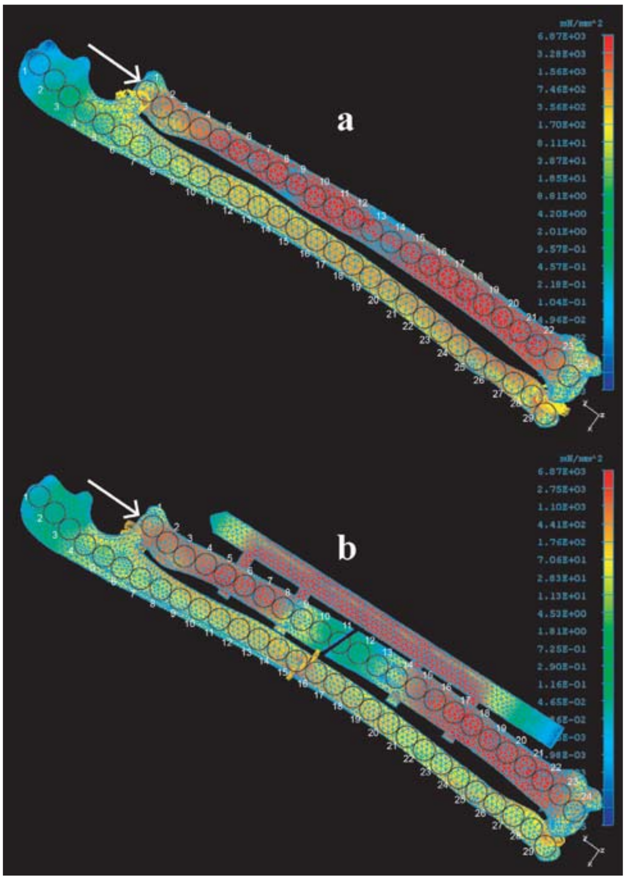

Fig. 4: Screenshots showing (a) the loaded model of the intact bones; (b) the loaded model of the fractured bones stabilized with an extramedullary IN; the circles and numbers identify the measuring points. The white vector marks the direction of pressure load, the colours visualize the amount of stress (red = high stress, blue = low stress).

Fig. 5: Photographs of the feline foreleg (obtained during the trial surgery) illustrating (a-c) the insertion of the IN fixed onto the positioning device according to minimally invasive surgery, and (d-f) the implantation during open treatment of the fractured bones using the IN like a plate: the dissected fracture ready for osteosynthesis (d), adjusting the IN onto the fractured radius (e), and the IN already fixed with screws onto the fractured radius (f).

Fig. 6: Lateral radiographic views of the feline antebrachium obtained before (a) and after (b) the trial surgery

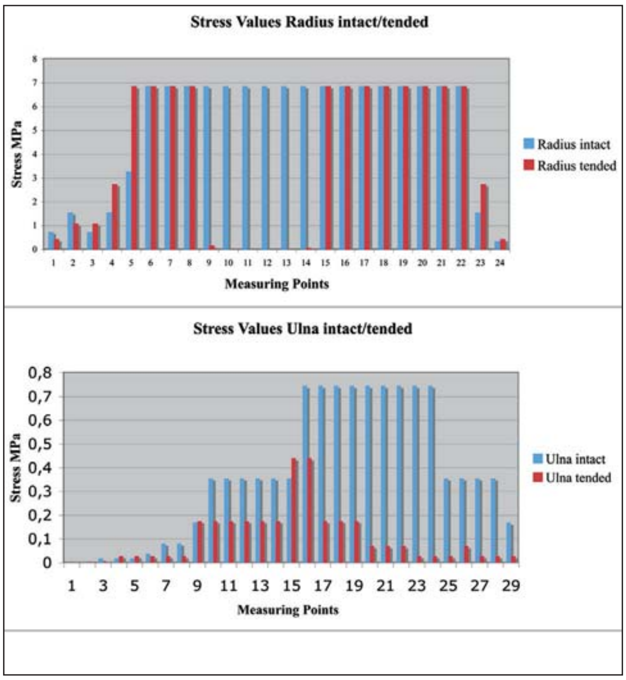

Fig. 7: Values of vertical stress of the intact (blue) and stabilized (red) bones; the bars represent stress magnitude.

the region of the olecranon, and ranged from 0.0283 MPa to 0.176 MPa in the proximal third. The stresses peaked in the fractured area in the middle third of the ulna, increasing from 0.176 MPa to 0.441 MPa and then decreasing back to 0.176 MPa. The stresses in the distal third of the broken ulna ranged from 0.0706 MPa to 0.0283 MPa, and remained at this value in the area of the caput radii with the processus styloideus.

Results of the trial surgery

The trial surgery was performed to assess the feasibility of fixing a fractured radius with an extramedullary IN. In the first step of the trial surgery we found that it was possible to position the IN in accordance with the criteria of minimally invasive surgery. We introduced and positioned the IN through a tiny incision made near the carpal joint on the craniomedial contour of the foreleg right above the processus styloideus radii, and fixed the screws through tiny incisions using the aiming device (Fig. 5a-c) after a closed reduction. In the second step, we showed that there were no difficulties in using the IN via a traditional approach. There were also no problems in fixing the IN onto the radius like a plate (Fig. 5d-f). Both scenarios demonstrated that an IN can be used to fix a fractured radius. To illustrate the situation of the fracture and the IN a X-ray was made before (Fig. 6a) and after (Fig. 6b) the trial surgery.

Discussion

FEM

Finite element modelling is a widely applied technique in many areas of science that also can be of benefit to medical science. It is very important to appropriately select the sample when digitizing the geometrical data, since only minor modifications are possible once the data point swarm has been transferred to the three-dimensional geometry suitable for FE meshing. In the present study, the feline radius and ulna prepared for image capture were carefully selected to represent average anatomical specimens according to the relevant literature (KÖNIG, 1992; NICKEL et al., 1992; SCHALLER, 1992; FREWEIN and VOLLMERHAUS, 1994), and the bones were prepared to present even and smooth surfaces. Careless groundwork could result in artifacts and unexplainable stresses and strains, leading to misinterpretations and false data. The FEMs of the radius and ulna presented here still need to be biomechanically validated based on strain gauges or similar technical investigations, but the stress distributions observed within the shafts of the bones and the close concordance in the stresses in the radius and ulna may well allow a positive interpretation of the stabilization results.

The finite element models

The FEMs of the feline radius and ulna represent a model of the feline antebrachial bones. The forces due to tendons, ligaments, and muscles were ignored, even though they would obviously modify the stress patterns (SHAHAR et al., 2003). However, the FEA results show that including only the bony structures provides reliable information on the mechanical behavior of the stabilization method of the extramedullary IN. Both the loaded and the stabilized radius and ulna exhibited stresses up to 6.87 MPa, leading to the conclusion that this kind of stabilization may represent a more than adequate method for the type of fracture investigated. These results demonstrate the advantages of additionally stabilizing muscles and other soft tissue. Our trial surgery also showed the feasibility of stabilizing a fractured radius and ulna. The main limitation of the trial surgery was that osteosynthesis employing either minimally invasive and standard approaches was only tested on a single foreleg of 1 euthanized cat. The next step is to validate the results of the FEA and trial surgery in in vivo animal experiments.

Clinical relevance

This study represents a very important first step in the long process of minimizing the number of animal trials needed in veterinary research. Subjects selected for clinical trials after completion of a FEA in osteosynthesis would no longer be exposed to the potential insecurity of a non-tested method. Other factors such as the material compatibility of metal implants, bone reaction to the screws, the surgical approach, and individual adaptations to anatomical variations are still reliant on clinical research, but our data have shown that nearly the entire load is transferred onto the IN, which should result in good healing of the fracture. As is usual in surgical repairs, only the fractured radius was stabilized with the IN because this bone is the principal weight-bearing bone of the foreleg (ROCHAT and PAYNE, 1993) and the ulna is adequately realigned when the radial fracture is reduced. This also minimizes the invasiveness due to the use of 2 screws in each fragment of the fracture. The data presented here demonstrate that the treatment of a diaphyseal fracture of the radius and ulna with an IN is similarly effective as an osteosynthesis using a plate as an external skeletal fixator.

Conclusion

The FEM created in this study allows calculation of stresses in the feline radius and ulna during the simulation of a 4-legged stance, with the resulting data showing that an extramedullary IN could be an appropriate tool for treating simple, not-dislocated diaphyseal fractures of the feline radius and ulna. This model could form the basis for future studies into the biomechanics of the feline antebrachium.

References

BOUDRIEAU, R.J. (2003): Fractures of the radius and ulna. In: SLATTER, D. (ed.): Textbook of small animal surgery. 3rd ed., Saunders, Philadelphia, p. 1953-1973.

FREWEIN, J., VOLLMERHAUS, B. (1994): Anatomie von Hund und Katze. Blackwell Wissenschafts-Verlag, Berlin, p.1994.

HINTERHOFER, C., STANEK, C., HAIDER, H. (2001): Finite element analysis (FEA) as a model to predict effects of farriery on the equine hoof. Equ. Vet. J. **33** (Suppl.), 58-62.

HINTERHOFER, C., FERGUSON, J.C., APPRICH, V., HAIDER, H., STANEK, C. (2005): A finite element model of the bovine claw under static load for evaluation of different flooring conditions. N. Z. Vet. J. **53**, 165-170.

HINTERHOFER, C., FERGUSON, J.C, APPRICH, V., HAIDER, H., STANEK. C. (2006): Slatted floors and solid floors: stress and strain on the bovine hoof claw capsule analyzed in finite element analysis. J. Dairy Sci. **89**, 155-162.

JOHNSON, K.A. (2003): Internal fracture fixation. In: SLATTER, D. (ed.): Textbook of small animal surgery. 3rd ed., Saunders, Philadelphia, p. 1807-1818.

KASTNER, J., HEIM, D., SALABERGER, D., SIMON, M. (2006): Advanced applications of computed tomography by combination of different methods. Proc. 9th Europ. Conf. Non-Destructive Testing, Berlin, p. 25-29.

KÖNIG, H.E. (1992): Anatomie der Katze mit Hinweisen für die tierärztliche Praxis. Fischer, Stuttgart.

LAUER, S., ARON, D.N., EVANS, M.D. (2000): Finite element method evaluation: articulations and diagonals in an 8-pin type 1B external skeletal fixator. Vet. Surg. **29**, 28-37.

MOORE, R., DAVIDS, N., FRIEDENBERG, R. (1969): Study of a biological model of membrane function by finite element analysis. Curr. Mod. Biol. **3**, 156-168.

MORGAN, E.F., BAYRAKTAR, H.H., KEAVENY, T.M. (2003): Trabecular bone modulus-density relationships depend on anatomic site. J. Biomech. **36**, 897-904.

NICKEL, R., SCHUMMER, A., SEIFERLE, E. (1992): Anatomie der Haustiere. 6. Aufl., Parey, Berlin.

PAO, Y.C., RITMAN, E.L., WOOD, E.H. (1974): Finite-element analysis of left ventricular myocardial stresses. J. Biomech. **7**, 469-477.

ROCHAT, M.C., PAYNE, J.T. (1993): Your options in managing long-bone fractures in dogs and cats. Vet. Med. **88**, 946-956.

RUDD, R.G., WHITEHAIR, J.G. (1992): Fractures of the radius and ulna. Vet. Clin. North Am. Small Anim. Pract. **22**, 135-148.

RUMPEL, G., SONDERHAUSEN, H.D. (1990): Strength of materials. In: BEITZ, W., KÜTTNER, K.H. (Hrsg.): Dubbel Taschenbuch für den Maschinenbau. 17. Aufl., Springer, Berlin, p. C 6.

SCHALLER, O. (1992): Illustrated veterinary anatomical nomenclature. Enke, Stuttgart.

SHAHAR, R., BANKS-SILLS, L., ELIASY, R. (2003): Stress and strain distribution in the intact femur: finite element analysis. Med. Engrg. Physics **25**, 387-395.

VNUK, D., PIRKIC, B., MATICIC, D., RADISIC, B., STEJSKAL, M., BABIC, T., KRESZINGER, M., LEMO, N. (2004) : Feline high-rise syndrome: 119 cases (1998–2001). J. Fel. Med. Surg. **6**, 305-312.

WENKEL, R., KAULFUSS, K.H. (2001): Frakturen bei Klein- und Heimtieren - Häufigkeiten, Klassifikation und Therapie. Kleintierpraxis **46**, 385-460.

Authors' address:

Mag. Georg R.F. Mahr, Dr. Karin Lorinson, Univ.Doz.Dr. Dragan Lorinson DECVS, Marktstraße 19, A-2331 Vösendorf; Mag. Georg R.F. Mahr, Dr. Christine Hinterhofer, Veterinärplatz 1, A-1210 Wien; Ing. Heinz Haider, Franz-Grill-Straße 5/Arsenal/Objekt 213, A-1030 Wien; D.I. Dr. Johann Kastner, Stelzhammerstraße 23, A-4600 Wels.

e-mail: tierarzt.mahr@chello.at